XIV International Conference on Computational Plasticity. Fundamentals and Applications
COMPLAS XIV
E. Oñate, D.R.J. Owen, D. Peric & M. Chiumenti (Eds)

REDUCTION OF THE MESH SIZE INFLUENCE ON THE RESULTS OF A LAGRANGIAN FINITE ELEMENT MACHINING MODEL

François DUCOBU, Edouard RIVIERE-LORPHEVRE and Enrico FILIPPI

University of Mons (UMONS), Faculty of Engineering (FPMs),
Machine Design and Production Engineering Lab
20 Place du Parc, B-7000 Mons, Belgium
e-mail: Francois.Ducobu@umons.ac.be, web page: http://http://www.geniemeca.fpms.ac.be/

Key words: Damage, Finite Element, Orthogonal Cutting, Mesh Dependence, Titanium Alloy Ti6Al4V

Abstract. Mesh dependence of the results of a finite element model are well known in many fields such as in structural design. This problem is however not much addressed in the literature for machining modelling although it is crucial for the quality of the results and the predictive aspect of the model. In this work, an orthogonal cutting model of the titanium alloy Ti6Al4V is exploited. The model formulation is Lagrangian and a damage criterion with eroding elements is used. A strong sensitivity of the results to the size of the elements is observed and the results do not converge when the size of the mesh decreases. To address this issue, a non-local damage criterion that reduces the mesh dependence of the results is introduced. The results show a strong decrease of their dependence to the size of the mesh. The recommendation is to use elements length that is not too far from the size of the grains of the material to avoid a dramatic increase of the computing time for very small elements and the absence of converged results for too large elements.

1 INTRODUCTION

The problem of mesh dependence of the results of a finite element model of machining is not much addressed in the literature. It is however crucial for the quality of the results and the predictive aspect of the model. Some works were identied on this subject in the literature, and particularly when segmented (also called saw-toothed) chips are formed. Karpat [1] observed that a decrease of the elements length decreases the width of the adiabatic shear band. Zhang et al. [2, 3] worked with four different elements sizes and studied their influence on the modelled cutting force. Larger elements lead to a cutting force value lower than the experimental value. Hortig ans Svendsen [4] noticed that a decrease in the elements length leads to a decrease of the adiabatic shear band width and a lower value of the cutting force. It is important to note that this last result is in contradiction of what Karpat [1] observed. Ambati and Yuan [5] concluded that the

cutting force is not dependent on the mesh density. They also observed that the width of the adiabatic shear band decreases with the size of the elements and that the chip becomes segmented although it was continuous for larger elements.

This literature review shows that a mesh dependence of the results can be highlighted but all the conclusions do not go in the same direction, and particularly for the cutting force. In this paper, an orthogonal cutting model of the titanium alloy Ti6Al4V is used to highlight and then reduce the influence of the mesh on the results when a segmented chip is formed.

2 FINITE ELEMENT MODEL PRESENTATION

The finite element model has previously been introduced by Ducobu et al. [6] to form realistic segmented Ti6Al4V chips, with the major difference that in this study damage properties are given to the whole workpiece. Its main characteristics are that it is a Lagrangian orthogonal cutting model developed with Abaqus. It is composed of a fixed workpiece and a tool moving horizontally at the cutting speed (Figure 1). The machined material, Ti6Al4V, is described by the TANH constitutive model [7], a modified Johnson-Cook material constitutive model [8] taking the strain softening into account. The cutting speed is 75 m/min and the uncut chip thickness is 0.28 mm. The tool has a rake angle of 15°, a clearance angle of 2° and a cutting edge radius of 20 µm. These cutting conditions experimentally lead to the formation of a segmented chip [9].

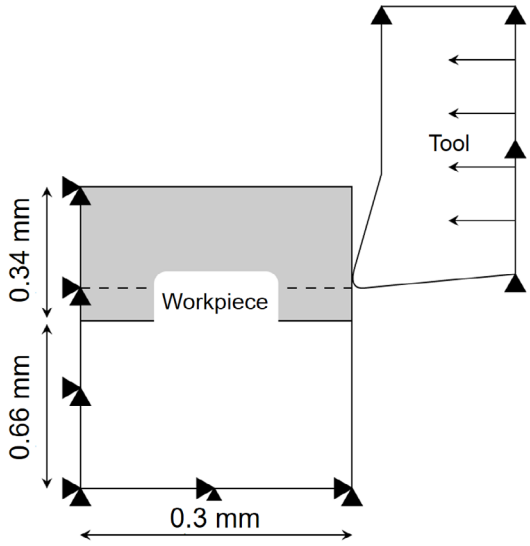

Figure 1: Configuration and boundary conditions of the model

With a Lagrangian formulation, a damage criterion has to be introduced to allow the chip to come off the workpiece. The adopted criterion is the temperature dependent tensile failure of Ti6Al4V [10, 11]. To limit the number of elements of the model and the computation time, only the first segment of the chip is modelled. This allows to consider a rather short workpiece (Figure 1). The size of the square elements ranges from 1 µm to

10 µm with a step of 1 µm. As shown in Figure 2, the computation time, with one Intel CPU at 3 GHz, increases much when the mesh density increases. For 84 µs of simulation time, the computation time is close to 500 h for a mesh of 1 µm while it is less than 5 minutes for a mesh of 10 µm.

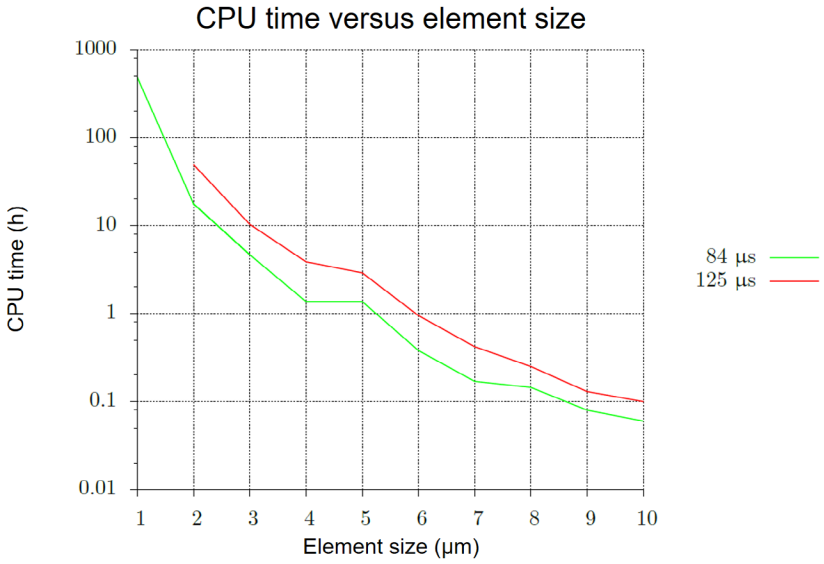

Figure 2: Evolution of the computation time with the mesh density (125 µs corresponds to the formation of the first segment, 84 µs is the maximum simulation time computed for 1 µm due to the very long computation time for that mesh size)

3 RESULTS FOR DIFFERENT MESH DENSITIES

Figure 3 presents the chip morphology for the 10 different meshes. They are globally close, except at 1 µm: a fracture propagates inside the primary shear zone very quickly (within 1 µs, the output frequency of the results) and a second fracture appears in the whole segment to cut it in two parts. When the mesh is 2 µm, the crack propagates quickly in the primary shear zone as well, but not in all of it and it takes longer than at 1 µm. Secondary fracture in the segment is also present at 2 µm and 3 µm. For all the meshes, the fracture propagates inside the primary shear zone, from the free surface of the chip to the tool radius.

As shown by Figure 4, the width of the adiabatic shear band decreases with the length of the elements. It is composed of 3-4 elements that are highly sheared. The decrease of the elements length leads to elements that are sooner highly sheared in the primary shear zone (the simulation time in Figure 4 decreases when the size of the elements decreases), which involves a quicker increase of the temperature.

The cutting and feed forces are presented in Figure 5 for the 10 meshes, together with the experimental reference of Sun et al. [9]. From 5 µm to 10 µm, the evolution and the values of the cutting force are close. Under 5 µm, the value of the first peak is reached sooner and its magnitude decreases. The fall of the cutting force is more abrupt (the

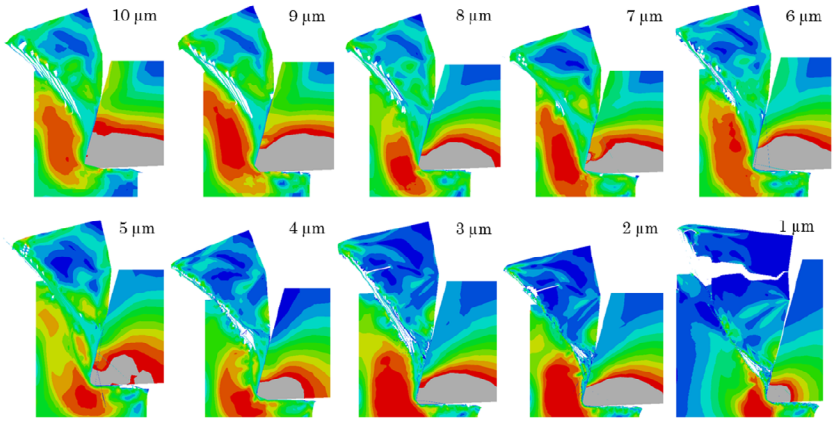

Figure 3: Chip morphology for different mesh densities (after 84 µs for elements of 1 µm and 125 µs from elements of 2 µm to elements of 10 µm)

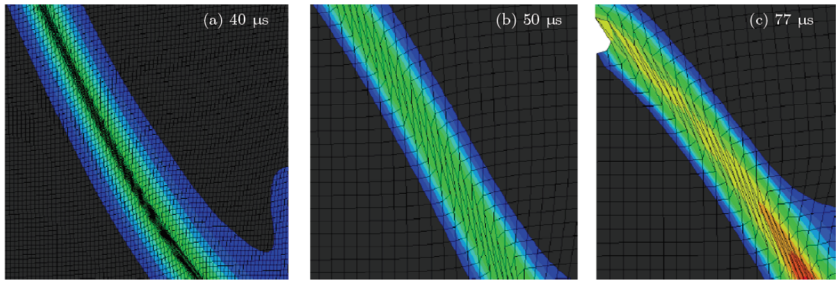

Figure 4: Width of the adiabatic shear band for an elements size of (a) 1 µm, (b) 5 µm and (c) 10 µm

width of the peak is smaller) and of a higher intensity (the minimal value is lower and it is reached sooner). This is due to the higher deformation of the elements and a higher temperature inducing a lower material strength. The fall is quicker and has a higher intensity because the fracture propagates quickly and is longer. For the feed force, it is the contrary (the force decreases when the elements length increases) but still with a significant mesh sensitivity.

In conclusions, the results do not converge when the mesh density increases, contrary to the expectations. The results remain close when the elements size is larger than 5 µm but then, if the elements size continues to decrease, they start to significantly diverge. This is particularly remarkable for the cutting force.

4 INTRODUCTION OF THE NON-LOCAL DAMAGE CRITERION

A significant mesh sensitivity of the results has been observed. This is mainly due to the introduction of damage and the softening of the material [12]. This leads to a strong localization inside the adiabatic shear band. To decrease this mesh sensitivity of the results, several methods can be found in the literature in other fields than metal cutting [12, 13]. Most of them consist of non-local methods that introduce an internal length. This internal length should be linked to the microstructure of the material (the

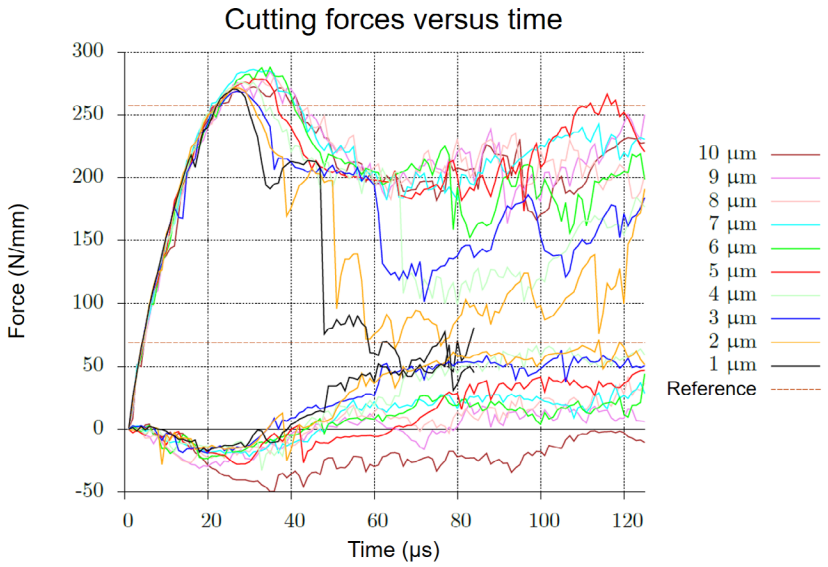

Figure 5: Cutting forces for the different mesh densities (experimental reference: Sun et al. [9])

grain size of Ti6Al4V is close to 5 µm) [12].

In Abaqus, the Johnson-Cook damage model, with initiation and propagation of damage, should allow to decrease the mesh dependence of the results once the damage initiation criterion has been reached in an element. This criterion has already been used in modelling of machining [14–16] and is composed of two steps (Figure 6 (a)). In the first step, the initiation of damage is computed in each element by

$$\omega = \sum \frac{\Delta\varepsilon}{\varepsilon_{D=0}} \tag{1}$$

With $\Delta\varepsilon$ the increment of equivalent plastic strain, $\varepsilon_{D=0}$ the equivalent plastic strain when damage is initiated ($\omega = 1$). It is computed by the Johnson-Cook damage model [17]

$$\begin{aligned} \varepsilon_{D=0} \quad = \quad & \left[D_1 + D_2 \ \exp\left(D_3 \ \sigma^*\right)\right] \left[1 + D_4 \ \ln \frac{\dot{\varepsilon}}{\dot{\varepsilon}_0}\right] \\ & \left[1 - D_5 \left(\frac{T - T_{room}}{T_{melt} - T_{room}}\right)\right] \end{aligned} \tag{2}$$

Where $\sigma^* = \frac{\sigma_m}{\sigma}$ is the stress triaxiality, σ_m is the mean stress and σ is the equivalent Von Mises stress. Variables D_1 to D_5 are model parameters and the other variables have the same meaning as for the Johnson-Cook material constitutive model: $\dot{\varepsilon}$ is the plastic strain rate, $\dot{\varepsilon}_0$ is the reference plastic strain rate, T_{room} is the room temperature and T_{melt} is the melting temperature.

After the initiation criterion has been reached, the damage propagates in a second step. The reduction of the mesh dependence to localization during damage evolution is carried out by introducing the fracture energy during crack propagation [18], G_f. It represents the stress-displacement relation rather than the stress-strain relation:

$$G_f = \int_{\varepsilon_{D=0}}^{\varepsilon_{D=1}} L_c \, \sigma \, \mathrm{d}\varepsilon = \int_0^{u_{D=1}} \sigma \, \mathrm{d}u \tag{3}$$

With L_c the element characteristic length and u the equivalent displacement. Before the onset of damage, $u = 0$ and after, $u = L_c \, \varepsilon$. In this model, the element characteristic length is the square root of the element surface [19]. The evolution of damage, D, is exponential:

$$D = 1 - \exp\left(- \int_0^{u_{D=1}} \frac{\sigma}{G_f} \, \mathrm{d}u \right) \tag{4}$$

When damage is initiated, D is equal to 0 and $\omega = 1$. At material failure, $D = 1$. When this second step is reached in an element, it is deleted which allows the chip to come off the workpiece and the crack can propagate.

Figure 6 compares schematically the behaviour of the material with the non-local damage criterion (a) and with the TANH constitutive model (b). In both cases, the objective is the same: taking into account the strain softening phenomenon that contributes to form a segmented chip.

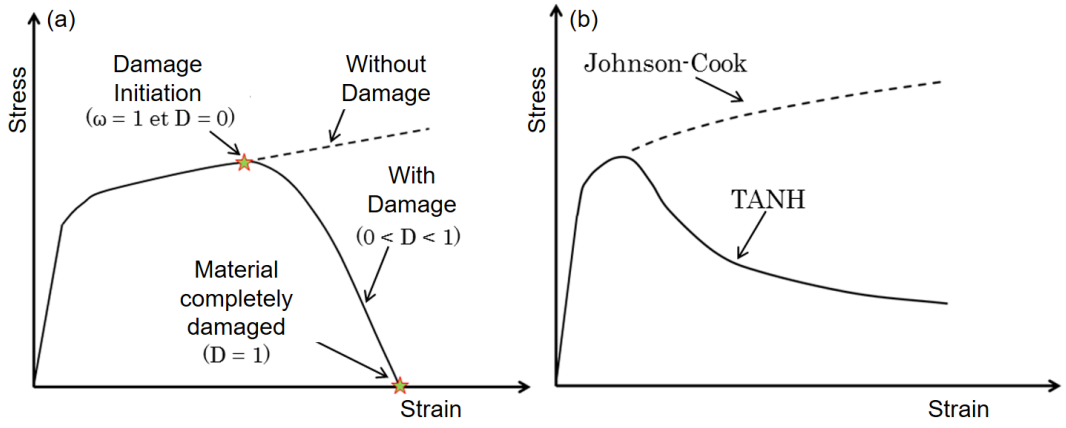

Figure 6: Behaviour of a material (a) with and without damage with the Johnson-Cook model, (b) without damage and the Johnson-Cook and TANH models

5 RESULTS WITH THE IMPROVED DAMAGE CRITERION

The chip morphology for the 10 meshes is presented in Figure 7. All the chips look similar. No damage localization, nor secondary crack are observed. A noticeable improvement is therefore brought. However, for 1 µm, some highly deformed elements are not deleted, which terminates prematurely the computation. The results for the width of the adiabatic shear band are improved as well. From 1 µm to 6 µm, its width remains constant and the number of elements inside of it grows as expected. Longer elements are too large to describe it.

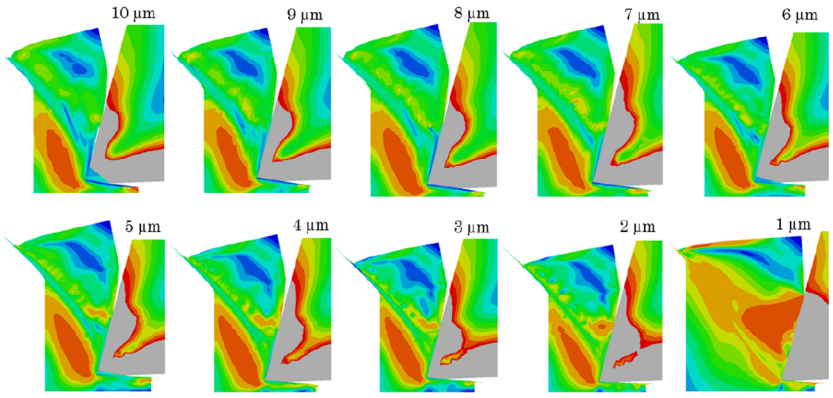

Figure 7: Chip morphology for different mesh densities after 125 µs (except 64 µs for 1 µm) with the non-local damage criterion

In Figure 8, it is seen that the cutting force has similar evolution and values for all the mesh densities up to 100 µs. Indeed, the initial effort rise is identical and the maximal value is reached at the same time. Only the 10 µm mesh has different values and high variations, which shows that the elements are too large. A similar observation is carried out for the feed force. The only difference is that the difference between the meshes begins at around 80 µs. In both cases, elements smaller than 4 µm lead to high forces variations after 100 µs.

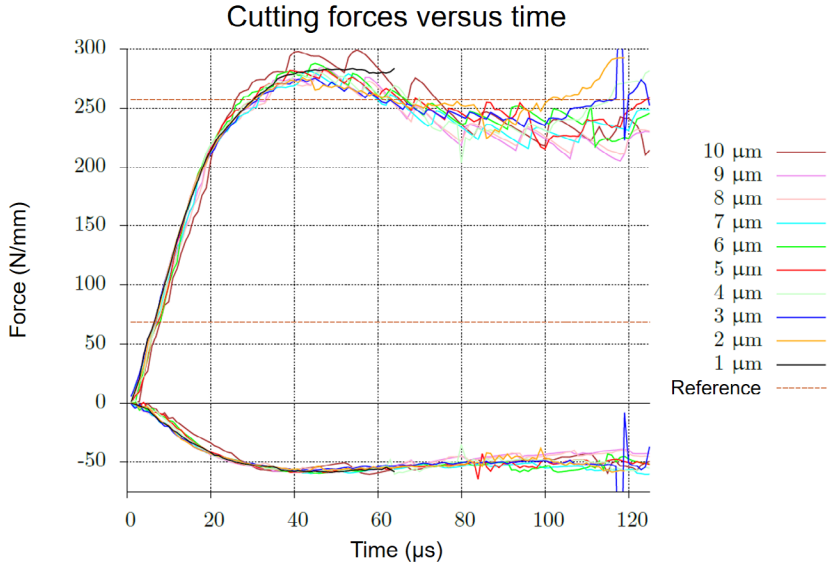

Figure 8: Cutting forces for the different mesh densities (experimental reference: Sun et al. [9]) with the non-local damage criterion

From the chip morphology results, the size of the elements should not be larger than 6 µm and small elements of 1 µm lead to highly deformed elements that are not deleted. For the forces, elements of 10 µm are too large and elements smaller to 4 µm should

not be used. In the end, although the mesh sensitivity is reduced, it has not completely disappeared and an element length of 5 µm would lead to good results in terms of chip morphology and cutting force.

6 CONCLUSIONS

A strong dependence of the results to the mesh density has been observed for the initial model with a local damage criterion. The reduction of this dependence has been carried out by introducing a non-local damage criterion based on the Johnson-Cook damage model. The results showed that localization of damage is reduced and that the sensitivity of the cutting forces to the mesh is significantly reduced. Some highly deformed elements that do not delete are however encountered, which can end prematurely the computation. An elements length of 5 µm is recommended, which is close to the grains size of the machined material.

REFERENCES

[1] Y. Karpat : Temperature dependent flow softening of titanium alloy Ti6Al4V: An investigation using finite element simulation of machining. *Journal of Materials Processing Technology*, 211:737–749, 2011.

[2] Y. Zhang, T. Mabrouki, D. Nelias et Y. Gong : FE-model for titanium alloy (Ti-6Al-4V) cutting based on the identification of limiting shear stress at tool-chip interface. *International Journal of Material Forming*, 4:11–23, 2011.

[3] Y.C. Zhang, T. Mabrouki, D.Nelias et Y.D.Gong : Chip formation in orthogonal cutting considering interface limiting shear stress and damage evolution based on fracture energy approach. *Finite Elements in Analysis and Design*, 47:850–863, 2011.

[4] C. Hortig et B. Svendsen : Simulation of chip formation during high-speed cutting. *Journal of Materials Processing Technology*, 186:66–76, 2007.

[5] R. Ambati et H. Yuan : FEM mesh-dependence in cutting process simulations. *International Journal of Advanced Manufacturing Technology*, 53:313–323, 2011.

[6] F. Ducobu, P.-J. Arrazola, E. Rivière-Lorphèvre et E. Filippi : Comparison of several behaviour laws intended to produce a realistic Ti6Al4V chip by finite elements modelling. *Key Engineering Materials*, 651–653:1197–1203, 2015.

[7] M. Calamaz, D. Coupard et F. Girot : A new material model for 2D numerical simulation of serrated chip formation when machining titanium alloy Ti-6Al-4V. *International Journal of Machine Tools and Manufacture*, 48:275–288, 2008.

[8] G.R. Johnson et W.H. Cook : A constitutive model and data for metals subjected to large strains, high strain rates and high temperatures. *Proceedings of the Seventh*

International Symposium on Ballistics, The Hague, The Netherlands, pages 541–547, 1983.

[9] S. Sun, M. Brandt et M.S. Dargusch : Characteristics of cutting forces and chip formation in machining of titanium alloys. *International Journal of Machine Tools and Manufacture*, 49:561–568, 2009.

[10] S. Lampman : Wrought titanium and titanium alloys, properties and selection: Nonferrous alloys and special-purpose materials. *ASM Handbook, ASM International*, 2:592–633, 1990.

[11] F. Ducobu, E. Rivière-Lorphèvre et E. Filippi : Material constitutive model and chip separation criterion influence on the modeling of Ti6Al4V machining with experimental validation in strictly orthogonal cutting condition. *International Journal of Mechanical Sciences*, 107:136–149, 2016.

[12] R.H.J. Peerlings, W.A.M. Brekelmans, R. de Borst et M.G.D. Geers : Gradient-enhanced damage modelling of fatigue failure. *Proceedings of the European Conference on ComputationalMechanics*, 1999.

[13] R. de Borst, M.G.D. Geers, R.H.J. Peerlings et A. Benallal : Some remarks on gradient and nonlocal damage theories. *Damage Mechanics in Engineering Materials*, 1998.

[14] T. Mabrouki, L. Deshayes, R. Ivester, J.-F. Rigal et K. Jurrens : Material modeling and experimental study of serrated chip morphology. *Proceedings of 7th CIRP International Workshop on Modeling of Machining Operations*, pages 53–66, 2004.

[15] T. Mabrouki et J.-F. Rigal : A contribution to a qualitative understanding of thermo-mechanical effects during chip formation in hard turning. *Journal of Materials Processing Technology*, 176:214–221, 2006.

[16] T. Mabrouki, F. Girardin, M. Asad et J.-F. Rigal : Numerical and experimental study of dry cutting for an aeronautic aluminium alloy (A2024-T351). *International Journal of Machine Tools and Manufacture*, 48:1187–1197, 2008.

[17] G.R. Johnson : Strength and fracture characteristics of a titanium alloy (.06ai, .04v) subjected to various strains, strain rates, temperatures and pressures. Rapport technique, NSWC TR 86-144, Dahlgren, VA, 1985.

[18] A. Hillerborg, M. Moder et P.E. Petersson : Analysis of crack formation and crack growth in concrete by means off racture mechanics and finite elements. *Cement and Concrete Research*, 6:773–782, 1976.

[19] H.K.S. : *Abaqus Analysis User's Manual, Version 6.14*. Dassault Systèmes, 2014.